COOPERATIVE TARGET TRACKING IN CONCENTRIC FORMATIONS

Lili Ma*

Abstract

This paper considers the problem of coordinating multiple unmanned aerial vehicles (UAVs) in a circular formation around a moving target. The main contribution is allowing for versatile formation patterns on the basis of the following components. Firstly, new uniform spacing control laws are proposed that spread the agents not necessarily over a full circle, but over a circular arc. Uniform spacing formation controllers are proposed, regulating either the separation distances or the separation angles between agents. Secondly, the use of virtual agents is proposed to allow for different radii in agents' orbits. Thirdly, a hierarchical combination of formation patterns is described. A Lyapunov analysis is conducted to study the stability characteristics. This paper also addresses the practical issue of collision avoidance that arises while UAVs are developing formations. An additional control component is added that repels agents to steer away from each other once they get too close. All UAVs have constant linear velocities. Control of the UAV is *via* its yaw rate. The proposed extensions to formation on a portion of a circle, circling on different radii for different agents, formation in local geometric shapes, and inter-vehicle collision avoidance, provide more complete solution to cooperative target tracking in concentric formations.

Key Words

Uniform spacing, virtual agent, hierarchical formation structure, inter-vehicle collision avoidance

1. Introduction

In recent years, multi-robot systems have been developed for a variety of applications. Coordinated systems are particularly interesting to the robotics community because they allow simple individual agents to achieve complex tasks in ways that are scalable, extensible, and robust to failures of individual agents [1]. Fundamental research works in coordinating a robotic network discuss issues such as collective and circular motions [2]–[8], time-varying and switching communication topologies [9], [10], time delays [1], [11], formation schemes [12]–[17], limited sensing [18]–[20], robot task assignment [21], [22], and Artificial Intelligent–based formation control [23], [24]. An application of these developed formation schemes is cooperative target tracking, where a group of agents are controlled to track a target while simultaneously maintaining formations. Cooperative control for tracking and enclosing of static and moving targets was reported in the literature [17], [25]–[34]. Different formation patterns have been brought into the context of cooperative tracking, including evenly spaced logarithmic spiral [17], balanced circular [31], uniform spacing [32], and triangular formations [33].

Cooperative target tracking while simultaneously maintaining formation has been achieved from slightly different perspectives. Starting from a formation pattern that is already achieved, one way is to control the centre of formation so that it tracks a given trajectory, *i.e.*, the trajectory of the moving target. It is commonly expected that coordinated control strategies that are generally designed with respect to (w.r.t.) a static centre will also show good performance when the target is moving. The work in [30] fits into this category, where a tracking control component is added into each robot's control input so that the formation centre can follow a moving target. The other approach is to add formation on top of an existing tracking scheme. The work described in this paper and our previous results in [35]–[37] belong to this category.

In this paper, the target moves on the ground with an unknown time-varying velocity. The unmanned aerial vehicles (UAVs) are commanded to orbit above the target performing simultaneous tracking and formation. Target tracking using one UAV has been solved in our previous work [38], where a tracking control law was designed to regulate the 2D horizontal range between the UAV and the target to a prescribed constant range. It is assumed that the target's position can be detected using an onboard camera, the target's velocity can be further estimated using an estimation scheme, and the relative altitude between the UAV and the target is available, *e.g.*, *via* geo-referencing the image captured by the camera with a given database [38]. The UAV is assumed to fly with constant linear velocity, and control of the UAV is *via* its yaw rate only.

Based on this tracking control that was designed for the single-UAV-target system, our results in [35]–[37] considered a multi-UAV-target tracking problem, *i.e.*, cooperative target tracking, by coordinating a group of UAVs to track the moving target in a balanced circular formation. All agents circle on the same orbit and spread evenly

* Department of Computer Engineering Technology, New York City College of Technology, City University of New York, New York, NY, USA; e-mail: LMa@citytech.cuny.edu

Recommended by Dr. Howard Li
(DOI: 10.2316/J.2021.206-0586)

around the full circle. Three formation controllers were adopted/designed in [35], [36], achieving the balanced circular formation under (1) all-to-all communication topology, (2) ring topology, and (3) cyclic pursuit, where each agent can get information from all the rest of the agents, from two other agents, or only from its "leading" agent, respectively.

Each UAV's yaw rate is designed as a combination (sum) of two control components, with one dedicated for tracking and the other for formation. These previous results [35]–[37] are focused on studying the feasibility of obtaining formation together with tracking, and were shown to be successful. The method of designing separate control component each having its own goal and using their combination to achieve an overall objective is effective [31], [32], [39]. A different formation pattern can be achieved simply by changing the formation control component alone.

This paper presents several new features, with the objective of obtaining more versatile formation patterns. Firstly, a new formation pattern, the uniform spacing formation, is obtained. Here, the uniform spacing formation refers to a formation pattern where all agents spread evenly over a portion of a circle, instead of the full circle. A chain-type communication topology is used, where two agents will be the "first" and the "last" in a platoon in a circular motion around the target with the rest of the agents spaced evenly in between. Secondly, different from our previous works where all agents circle on the same orbit, agents can now be controlled to circle on different orbits (circles of different radii). This is more suitable when agents need to perform different missions. For instance, the inner agents monitor the target while the outer agents protect the inner agents against possible attacks [7]. Uniform spacing controllers that regulate either the separation distances between a pair of agents or the separation angles between them w.r.t. the target are proposed for both cases, *i.e.*, circling on the same orbit or different orbits. For simplicity, the desired value, no matter for separation distance or separation angle, is assumed to be constant. When agents circle on different orbits, formation control laws will use information pertaining to a "virtual agent" instead of the actual agent itself. Thirdly, a two-layer hierarchical formation structure is further applied, allowing different subgroups to select different formation control laws. More versatile formation patterns can thus be achieved on the basis of all these features, including our existing results (tracking [38] and balanced circular formation [35]–[37]) and the new results in this paper (uniform spacing formations on the same orbit or different orbits regulating separation distances or angles, hierarchy). Fourthly, the practical issue of inter-vehicle collision avoidance is tackled, by adding a third control component to each UAV's input. This term repels agents to steer away from each other once they get close. The combination of Attraction (another way of saying tracking), Alignment (formation), and Avoidance (collision avoidance) provides a more complete solution to cooperative target tracking in concentric formations.

Results in this paper allow selection of the formation pattern among several candidates (balanced circular, uniform spacing, and their combinations). This feature is useful when considering a practical application with physical limitations. One such limitation is limited communication range. If the communication range does not allow all agents to separate so far away from each other, the uniform spacing formation can be more appropriate.

Among other existing results in the literature, the work in [39] is very relevant to ours. Both address vision-based tracking of a moving ground target by coordinating a group of UAVs. Our study is different from [39] in at least two aspects. Firstly, the achieved formation in [39] is a balanced circular formation. Secondly, the control inputs in [39] include both linear and angular velocities: tracking is achieved by altering each UAV's yaw rate and formation is obtained by adjusting each UAV's linear velocity (speed). Instead, in this paper, more versatile concentric formation patterns are obtained, including uniform spacing, balanced circular, and their combinations. All UAVs have constant linear velocities. Control is *via* each UAV's yaw rate only. This control strategy of altering yaw rate is more ready to be applied because most UAVs have low-level air speed hold controller. Implementation of yaw rate controllers does not impose additional requirements. Another important reference is [32], where the uniform spacing formation was achieved. However, theoretical analysis in [32] was only performed for a stationary target. While in our work, theoretical study of simultaneous tracking of a moving target and formation in the uniform spacing pattern is performed (Proposition 1).

In summary, the purpose of this work is to develop techniques that lead to versatile formation patterns for cooperative target tracking. The contributions of this paper include: (1) proposing a new bearing-angle-based coordination control law that realizes uniform spacing formation; (2) designing a method to command all UAVs to circle on different orbits with the introduction of virtual agents; (3) implementing a hierarchical structure such that different formation patterns can be specified for different layers; and (4) addressing the issue of inter-vehicle collision by adding one more control component that repels agents to steer away from each other once they get too close.

The paper is organized as follows. Section 2 presents the new uniform spacing formations where agents circle on a portion of a circle instead of a full circle. Using "virtual agent", formation controllers are presented in Section 3 that circle agents on different orbits around the moving target. By further adoption of a two-layer hierarchical formation structure that allows subgroups on different layers to select different formation schemes, more versatile formation patterns are achieved as shown in Section 4. The practical issue of inter-vehicle collision avoidance is addressed in Section 5. Simulation examples are given in Section 6. More discussions of research results and findings are provided in Section 7. Conclusions are described in Section 8.

2. Uniform Spacing Formations

Suppose there is a group of n UAVs (agents) moving at constant speeds. We use $\mathcal{N}_i$ to denote the neighbourhood

set of the agent i, which is the set of UAVs whose position(s) can be obtained by the agent i *via* communication. To achieve uniform spacing formation (Fig. 2(b)), a chain-type communication topology is used, where one agent does not "pursue" any agent and the rest of the agents each pursues its "leading" agent. Let k denote the index of the above-mentioned "particular" agent that does not "seek" anyone else. For agent k, its neighbourhood set is empty. For agent i in the rest of the agents, $\mathcal{N}_i$ contains only its "leading" agent, *i.e.*, agent $i+1$ (modulo n). The chain-type communication topology is like a cyclic pursuit strategy with a broken link between agents k and $k+1$ (modulo n). When coordinating the multi-UAV system to track a moving target:

- Tracking: Each UAV will track the moving ground target by maintaining a desired 2D horizontal range in between. The 2D range is given as a constant, denoted by ρ_d.
- Formations: New formation patterns, *i.e.*, the uniform spacing formations, are obtained. Either the relative separation distances or the separation angles between two adjacent (successive) agents can be regulated to approach a specified value. We use d_s and ϕ_s to denote the desired separation distance and the desired separation angle, respectively. Here, the subscript s denotes "separation". If all agents circle on the same orbit, then a constant separation distance is equivalent to a constant separation angle. When agents circle on different orbits, these two are slightly different. They are both uniform in certain sense, with one in distance spacing and the other in angular spacing.
- Control input: All UAVs are assumed to have constant linear velocities. Each UAV's linear velocity does not change over time. UAVs that are on the same orbit have the same linear velocity. Control of the UAVs are *via* their yaw rates only.
- Target information: The target moves on the ground with an unknown velocity. Each UAV is assumed to be equipped with an onboard camera, from where visual measurements of the target can be obtained by an image processing function. The relative altitude between each UAV and the target is assumed to be available, for example, *via* geo-referencing the image captured by the camera with a given database [38]. Estimation of the target's velocity, either constant or time-varying, is described in [38] and is not elaborated here.

2.1 Problem Formulation and Tracking Control Law

This section presents the problem formation. To make this paper self-contained, we start by briefly describing our previously designed tracking control law that maintains the 2D horizontal range between each UAV and the target to a prescribed range reference [35], [38], [39]. To maximize fuel efficiency, each UAV maintains a constant speed (linear velocity). Further, we assume that all UAVs fly at a fixed height and there is no wind. Figure 1 shows a 2D illustration of the UAV-target tracking problem.

The kinematic equations for the ith UAV tracking a ground target are shown below [35]–[38]:

$$\begin{cases} \dot{\rho}_i(t) = -V_{g,i}(t)\sin\eta_i(t) + V_t(t)\sin[\psi_t(t) - (\psi_i(t) - \eta_i(t))] = \zeta_{1i}(\omega_i(t))\sin(\eta_i + \zeta_{2i}(\omega_i(t))) \\ \dot{\eta}_i(t) = -\frac{V_{g,i}(t)\cos\eta_i(t) - V_t(t)\cos[\psi_t(t) - (\psi_i(t) - \eta_i(t))]}{\rho_i(t)} + \dot{\psi}_i(t) \end{cases} \tag{1}$$

where:

$$\begin{aligned} &\zeta_{1i}(\boldsymbol{\omega}(t)) = \text{sign}(\rho_{si}(t))\sqrt{\rho_{si}^2(t) + \rho_{ci}^2(t)}, \qquad \zeta_{2i}(\omega(t)) = \tan^{-1}\left(\frac{\rho_{ci}(t)}{\rho_{si}(t)}\right) \\ &\rho_{si}(t) = -V_{g,i}(t) + V_t(t)\cos(\psi_t(t) - \psi_i(t)), \quad \rho_{ci}(t) = V_t(t)\sin(\psi_t(t) - \psi_i(t)) \end{aligned} \tag{2}$$

and where:

- $\dot{\psi}_i(t)$ denotes the UAV's yaw rate and is the control input.
- $\lambda_i(t)$ denotes the line-of-sight angle.
- $\rho_i(t)$ denotes the 2D horizontal range between the ith UAV and the target.
- $V_{g,i}(t)$ denotes the projection of the ith UAV's velocity onto the horizontal plane.
- $\psi_i(t)$ denotes the ith UAV's heading.
- $\eta_i(t)$ denotes the angle between the ith UAV's velocity and the vector perpendicular to the line-of-sight.
- $V_t(t)$ and $\psi_t(t)$ are the amplitude and orientation of the target's velocity $\boldsymbol{\omega}(t) = [\omega_1(t), \omega_2(t)]^\top$, where $\omega_1(t)$ and $\omega_2(t)$ are the target's velocity vectors along the x-axis and the y-axis, respectively. That is, $\omega_1(t) = V_t(t)\sin\psi_t(t), \omega_2(t) = V_t(t)\cos\psi_t(t)$, and

$$V_t(t) = \sqrt{\omega_1^2(t) + \omega_2^2(t)}, \quad \psi_t(t) = \tan^{-1}\left(\frac{\omega_1(t)}{\omega_2(t)}\right) \tag{3}$$

Assume that the linear velocities $V_{g,i}(t)$ of all UAVs are constant and $V_{g,i}(t) \gg V_t(t)$. Our previous results on cooperative target tracking coordinated the multi-UAV system in a way that all the n UAVs track the target with a prescribed range distance in a balanced circular formation (with all agents distributed evenly around a circle whose centre resides in the moving target). The control input

to each UAV (the yaw rate $\dot{\psi}_i(t)$) was designed as a combination of several individual control components, each having its own goal. Let $u_{it}(t)$ and $u_{ic}(t)$ denote a tracking and a coordination control component, respectively. The control input to each agent is [35]–[37]:

$$\dot{\psi}_i(t) = u_{it}(t) + u_{ic}(t) \tag{4}$$

This approach makes it possible to obtain a different formation pattern simply by modifying the coordination control component alone. Additional control component(s) can also be incorporated. In Section 5, a collision-avoidance control component is added to avoid inter-vehicle collisions.

The tracking control law $u_{it}(t)$ in (4) was designed in [38] and shown below. It regulates the 2D horizontal range $\rho_i(t)$ between the ith UAV and the moving target to a specified constant ρ_d [38]:

$$\begin{cases} u_{it}(t) = \dfrac{V_{g,i}(t)\cos\eta_i(t) - \hat{V}_{ti}(t)\cos[\hat{\psi}_{ti}(t) - (\psi_i(t) - \eta_i(t))]}{\rho_i(t)} - k_2(\eta_i(t) - \eta_{di}(t)) \\ \eta_{di}(t) = \sin^{-1}\left(\frac{-k_1(\rho_i(t)-\rho_d)}{\zeta_{1i}(\omega_{ei}(t))}\right) - \zeta_{2i}\left(\boldsymbol{\omega}_{ei}(t)\right) \end{cases} \tag{5}$$

where k_1, k_2 are design gains. The signals $\hat{V}_{ti}(t)$, $\hat{\psi}_{ti}(t)$, and $\boldsymbol{\omega}_{ei}(t)$ denote estimates of $V_{ti}(t)$, $\psi_{ti}(t)$, and $\boldsymbol{\omega}_i(t)$, obtained by the ith UAV. An estimation scheme was described in [38] and is not repeated here.

2.2 Formation Control Laws

Instead of spreading all agents evenly around a full circle as in balanced circular formation (Fig. 2(a)), formation control laws that spread all agents evenly over a *portion* of a circle are proposed (Fig. 2(b)). This formation pattern was referred to as uniform spacing formation [32]. The yaw rate of each agent still takes the form of (4), where the tracking control remains the same (still (5)) but the formation control will be replaced by a different function.

We first describe the communication topology for the uniform spacing formations. Consider a variation of the cyclic pursuit strategy, where all UAVs, except one, still communicate in the cyclic pursuit manner. The particular agent that does not "seek" any other agents performs only tracking, *i.e.*, its coordination control component is zero. We refer to this communication topology the chain-type communication topology. The chain-type topology has a broken link compared with the cyclic pursuit.

Uniform spacing formation has been achieved in [32], where the formation control law was designed to use both the relative distances and the relative bearing angles among agents. Let $d_{ij}(t)$ and $\beta_{ij}(t) \in [-\pi, \pi]$ denote the linear and the angular distance between two consecutive agents, i and j. The signal $\beta_{ij}(t)$ is also called the relative bearing angle [31], [40] (Fig. 3). An adapted version of the coordination control law in [32] that fits into the chain-type communication topology takes the following form:

$$u_{ic}(t) = \begin{cases} 0, & i = k \\ -k_v\beta_{i(i+1)}(t)\ln\left(\frac{(c_v-1)d_{i(i+1)}(t)+d_s}{c_v d_s}\right), & i \neq k \end{cases} \tag{6}$$

where $k_v > 0, c_v > 1$, and k denotes the index of the above-mentioned "particular" agent that does not "seek" anyone else. d_s in (6) is the desired separation distance.

When circling on the same orbit, the relative bearing angle can be a good indicator of the relative distance (see Fig. 3). We thus propose a coordination scheme that is a function of only the relative bearing angle(s). This is also motivated by our cyclic pursuit coordination controller in [35] that achieved the balanced circular formation by controlling $\cos\beta_{i(i+1)}(t)$ to approach $\cos(\pi/n)$. Now, by controlling $\cos\beta_{i(i+1)}(t)$ to approach a function of the

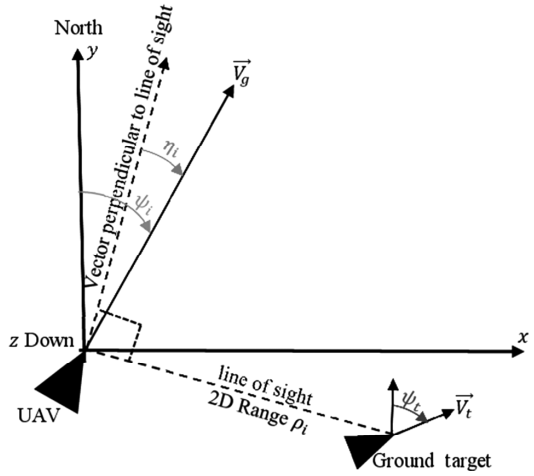

Figure 1. Relative kinematics of UAV-target motion on a projected 2D plane.

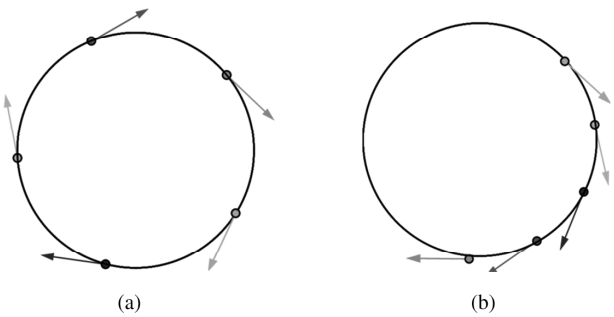

Figure 2. (a) Balanced circular versus (b) uniform spacing formations.

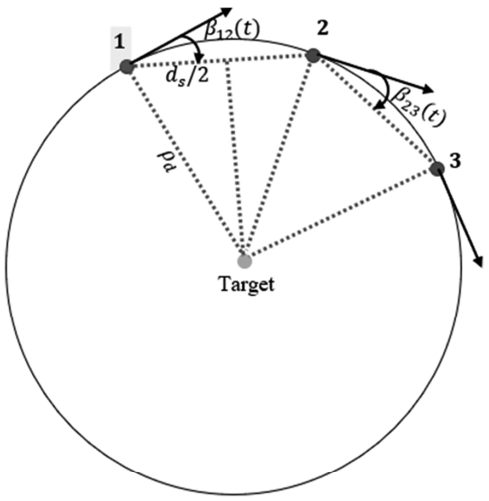

Figure 3. Illustration of relative bearing angle $\beta_{ij}(t)$.

desired separation distance d_s, the uniform spacing formation can be achieved. When satisfactory tracking has been obtained, each UAV's velocity vector becomes perpendicular to the vector pointing from the target to the UAV. When the 2D range referee is constant or piecewise-constant, we propose the following coordination control:

$$u_{ic}(t) = \begin{cases} 0, & i = k \\ -\kappa(\cos\beta_{i(i+1)}(t) - \cos\beta_0),\ i \neq k, \kappa > 0 \end{cases} \quad (7)$$

where

$$\beta_0 = \frac{\pi}{2} - \cos^{-1}\left(\frac{d_s}{2\rho_d}\right) \quad (8)$$

As a result, the separation angle between two successive agents is

$$\phi_s = 2\sin^{-1}\left(\frac{d_s}{2\rho_d}\right) \quad \text{or} \quad \phi_s = 2\pi - 2\sin^{-1}\left(\frac{d_s}{2\rho_d}\right) \quad (9)$$

Notice that the communication topology for (7) is still the chain-type communication topology.

When all agents circle on the same orbit, selecting β_0 according to (8) ensures that the relative distance between two consecutive agents approaches the specified d_s. Simulation results show that both coordination control laws (6) and (7) obtain similar performance under this circumstance. Our proposed controller (7) has a much simpler form and is consistent with our existing coordination control laws that are all expressed as functions of relative bearing angles. As the bearing angle can be measured in the local coordinate frame of each agent, it provides a possibility to still maintain formation even during communication loss. In which case, local measurements and estimates can be used to replace the expected exchanged information when they become unavailable.

The following result is achieved obtaining the uniform spacing formation under the chain-type communication topology by altering $\hat{\psi}_i(t)$:

Proposition 1. *Consider the system of* n *agents with kinematic equations given in* (1). *Suppose that the communication topology is a variation of the cyclic pursuit strategy where one agent does not "seek" any other agents with the rest of the agents behaving in the cyclic pursuit manner. Applying the control law* (4) *with the tracking control component* (5) *and the coordination control component* (7), *the* n*-agent system is globally uniformly ultimately bounded with both tracking and coordination bounds as* $|\rho_i(t) - \rho_d(t)| \leq \varepsilon_1$ *and* $|\cos\beta_{i(i+1)}(t) - \cos\beta_0| \leq \varepsilon_2$, *for* $i = 1, 2, \ldots, n$. *Expressions of* $\varepsilon_1, \varepsilon_2$ *are in* (27), (34).

Proof of Proposition 1 follows that in [37] and is not provided here due to page limit.

3. Formation Control Laws for Circling Agents on Different Orbits

The formation controllers in Section 2.2 and references [35]–[37] control all agents to circle on one orbit (the same orbit). For more flexibility and versatility, one would want all agents to be able to circle on different orbits. This section describes the modifications and arrangements needed to make this happen.

Start by considering target tracking. When all UAVs are commanded to orbit on the same circle, the 2D range reference is the same for all UAVs and is denoted by ρ_d so far. Accordingly, the linear velocities $V_{g,i}$ are the same for all UAVs. To circle UAVs on different orbits, the range references will be different. As a result, UAVs' linear velocities, which are the same before, need to be different. Let $\rho_{d,i}$ and $V_{g,i}$ denote the prescribed range reference and linear velocity of agent i. Using agents i and j as an example, the relationship between their linear velocities and 2D range references needs to satisfy:

$$\frac{V_{g,i}}{V_{g,j}} = \frac{\rho_{d,i}}{\rho_{d,j}} \quad (10)$$

For coordination, our approach to coordinate all agents to circle on different orbits is to refer to virtual agent(s). Suppose agent i needs information from agent j to achieve coordination. Instead of using agent j's information, agent i will use information from a virtual agent that represents agent j but orbits on the same orbit as agent i. This virtual agent, denoted by the big dot in Fig. 4, lies in the intersection of agent i's own orbit and the line connecting the target and the actual agent j. That is, the virtual agent is the projection of agent j onto agent i's orbit w.r.t. the target. No modification is needed to an existing communication topology. No additional information exchange among agents is required. Based on the target's position (measured/estimated by each agent), each agent's position (known from the agent's onboard sensor), and the neighbouring agent's position (obtained *via* information exchange), the position of the virtual agent can be computed.

Let $[x_i(t), y_i(t)]^\top$ be the agent i's Cartesian coordinate in the world frame. Suppose that the coordination control law of agent i requires information of agent j. Instead

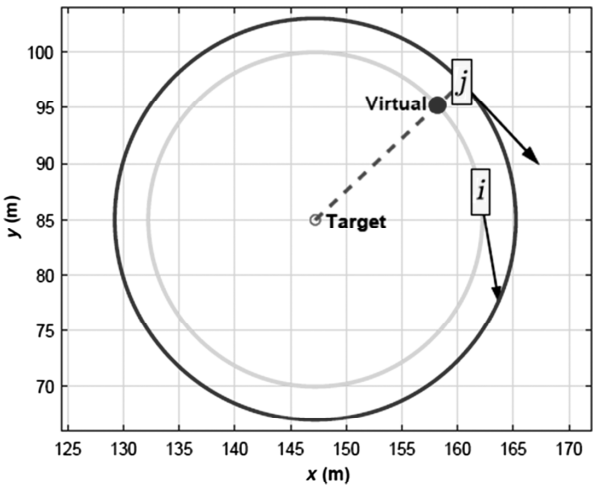

Figure 4. Virtual agent representing agent j used by agent i.

of using agent j's information $[x_j(t), y_j(t)]^\top$ directly, a virtual agent will be first computed and then used. The virtual agent does not necessarily have a speed associated with it. It is its relative position (distance or separation angle) w.r.t. agent i that matters. The coordinates of this virtual agent, denoted by $[\tilde{x}_i(t), \tilde{y}(t)]^\top$, are computed as:

$$\begin{aligned} \tilde{x}_j(t) &= \frac{\rho_{d,i}}{\rho_{d,j}}\left(x_j(t) - x_t(t)\right) + x_t(t), \\ \tilde{y}_j(t) &= \frac{\rho_{d,i}}{\rho_{d,j}}(y_j(t) - y_t(t)) + y_t(t) \end{aligned} \tag{11}$$

Letting $\tilde{\beta}_{i,j}(t) \in [-\pi, \pi]$ denote the relative bearing angle between agent i and the virtual agent representing agent j, it can be computed as:

$$\tilde{\beta}_{i,j}(t) = \tan^{-1}\left(\frac{\tilde{y}_j(t) - y_i(t)}{\tilde{x}_j(t) - x_i(t)}\right) - \theta_i(t) \tag{12}$$

where $\theta_i(t)$ is the angle of the ith agent's velocity vector w.r.t. the x-axis, which can be computed as $\theta_i(t) = \frac{\pi}{2} - \psi_i(t)$.

To extend to the scenario of circling on different orbits, we refine the definition of uniform spacing to have either desired distance spacing or desired angular spacing between two agents. In the case of spacing in distance, the separation distances between two consecutive agents will be regulated to the desired value. For spacing in angular distance, the separation angles between each two consecutive agents w.r.t. the target are regulated to the desired value, regardless of the orbits they are on. Under this extension, the case of circling on the same orbit becomes a special case with all orbits reducing to one, where constant relative distance is equivalent to constant separation angle, and the virtual agent representing agent j is the agent j itself. These are no longer true for circling on different orbits. To circle on different orbits, our formation control laws, which were all designed as functions of relative bearing angles $\beta_{i,j}(t)$ referring to the actual agents, will be modified to use relative bearing angles $\tilde{\beta}_{i,j}(t)$ referring to the virtual agents.

To be specific, consider the balanced circular formation. Simply by replacing $\beta_{i,j}(t)$ with $\tilde{\beta}_{i,j}(t)$, the balanced circular formation can be obtained in a straightforward manner for the case of circling on different orbits. Particularly, the three formation control laws in [35] are modified to be:

- Achieving balanced circular formation under all-to-all:

$$u_{ic}(t) = -\kappa \sum_{j=1, j\neq i}^{n} \cos\tilde{\beta}_{ij}(t), \kappa > 0 \tag{13}$$

- Achieving balanced circular formation under ring:

$$u_{ic}(t) = -\kappa\Big[\cos\tilde{\beta}_{i(i+1)}(t) + \cos\tilde{\beta}_{i(i-1)}(t)\Big], \kappa > 0 \tag{14}$$

- Achieving balanced circular formation under cyclic:

$$u_{ic}(t) = -\kappa\Big[\cos\tilde{\beta}_{i(i+1)}(t) - \cos\left(\frac{\pi}{n}\right)\Big], \kappa > 0 \tag{15}$$

For uniform spacing formations, controller (6) is modified to be:

$$u_{ic}(t) = \begin{cases} 0, & i = k \\ -k_v\tilde{\beta}_{i(i+1)}(t)\ln\left(\frac{(c_v-1)d_{i(i+1)}(t)+d_s}{c_v d_s}\right), & i \neq k \end{cases} \tag{16}$$

Our coordination controller (7) is a function of both $\beta_{i(i+1)}(t)$ and β_0. Similarly, $\beta_{i(i+1)}(t)$ will be replaced by $\tilde{\beta}_{i(i+1)}(t)$. For circling on different orbits, it is not convenient to use d_s to specify the desired separation angle, as in (8). Instead, the desired separation angle, denoted by ϕ_s, will be specified directly. Our formation controller (7) is modified as shown below with $\beta_0 = \phi_s/2$:

$$u_{ic}(t) = \begin{cases} 0, & i = k \\ -\kappa(\cos\tilde{\beta}_{i(i+1)}(t) - \cos\beta_0), & i \neq k, \kappa > 0 \end{cases} \tag{17}$$

In certain circumstance, one coordination control law might be more convenient than the other. For instance, when the formation is specified literally using relative distance(s), the coordination control laws (6) or (16) might be more convenient. If the formation is concerned with relative angular distance, the coordination control laws (7) or (17) might suit better.

4. Concentric Formations with Local Geometric Shapes

So far, we have achieved two formation patterns (balanced circular in [35], [36] and uniform spacing in Sections 2.2 and 3) and allowed agents to circle on either the same orbit or different orbits. In the context of concentric formations, we would like to generate more versatile formations, such as formations with local geometric shapes. Clearly, combinations of circular and/or uniform formations are more

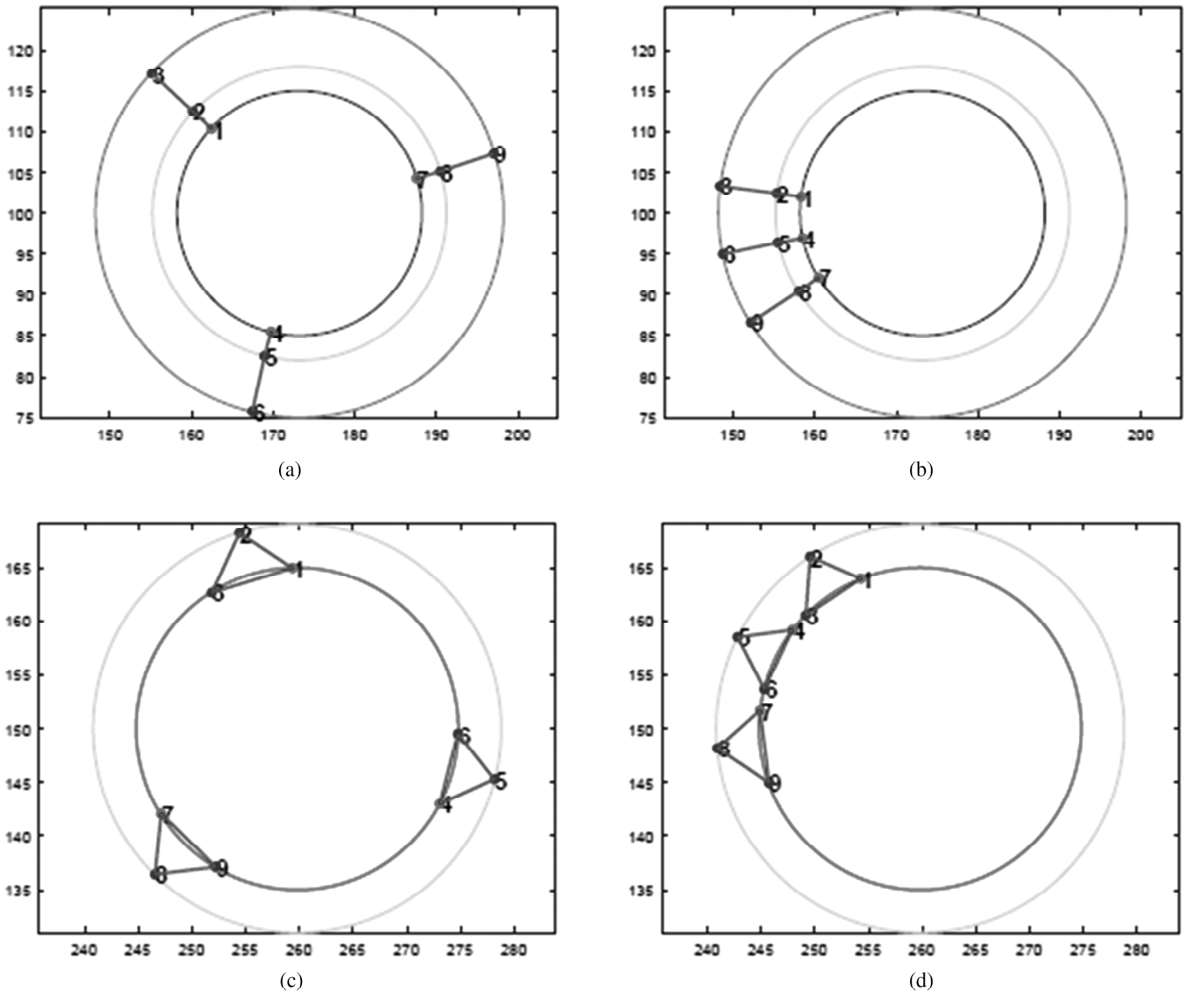

Figure 5. Formations in local geometric shapes (straight lines and triangles): (a) balanced-line; (b) uniform-line; (c) balanced-triangle; and (d) uniform-triangle.

versatile than one fixed pattern. This is done by utilizing existing features (tracking, formation in different patterns, circling on different orbits), with the help of a hierarchical formation structure [41]–[44]. The simplest hierarchical scheme, the two-layer hierarchical structure, can be described as follows. A collection of n agents is divided into n_2 subgroups, each containing n_1 agents ($n_1 \times n_2 = n$). The local control strategy is chosen such that the agents within each subgroup can be commanded to achieve certain formation pattern [41]. In [44], a two-layer hybrid pursuit system was described, where cyclic pursuit strategy was considered at the higher layer (the first layer) and chain-like communication topology was used at the lower layer (the second layer).

The concept of hierarchy is now applied to cooperative target tracking. The idea of hierarchy allows different subgroups to select different formation laws that are already known to be stable. Similar to [44], a two-layer hierarchical formation structure is used. The first layer can be set to achieve either the balanced circular or the uniform spacing formation. The second layer can be set to achieve the uniform spacing formation by specifying either a desired separation distance or angle. Two examples are given below to demonstrate how versatile patterns are achieved by determining the 2D range references of the agents (same or different) and the formation pattern on each layer (balanced circular or uniform spacing).

The first example achieves concentric formations with local geometric shapes in straight lines:

(1) The agents {1, 4, 7}, {2, 5, 8}, and {3, 6, 9} are assigned to be on the inner, middle, and outer orbits, respectively, by specifying their 2D range references to be {15, 18, 25} (m). Correspondingly, the UAVs' linear velocities are set to be {30, 36, 50} (m/s), satisfying the relationship in (10).

(2) On the first layer, the balanced circular formation is used for agents {1, 4, 7}, which lie on the inner circle. On the second layer, a uniform spacing formation is used inside each subgroup. There are three subgroups: {1, 2, 3}, {4, 5, 6}, and {7, 8, 9}. The agent that is involved in formation on the first layer works as "leader" of its subgroup. As the intended geometric shape is in straight line and the radial differences between each two adjacent orbits can be different, it is more convenient to use (7) with $\beta_0 = \pi/2$. Actual agents are used when obtaining bearing angles $\beta_{i(i+1)}(t)$. The formation pattern is shown in Fig. 5(a).

(3) Simply changing the formation pattern on the first layer from the balanced circular to the uniform spacing pattern, an overall uniform spacing formation is achieved with local geometric shapes in straight lines. The formation pattern is shown in Fig. 5(b).

The second example achieves concentric formations with local geometric shapes in triangles:

(1) The agents {1, 3, 4, 6, 7, 9} are assigned to circle on the inner orbit. All other agents circle on the outer orbit. The 2D range references $\rho_{d,i}$ are {15, 19} (m), which requires UAVs' linear velocities to be {30, 38} (m/s).
(2) Agents {1, 4, 7} are used to form a balanced circular formation on the first layer. On the second layer, a uniform spacing formation is used. To achieve local shapes in triangles, it is convenient to use (16), which regulates distances directly. Virtual agents are used. The achieved formation pattern is shown in Fig. 5(c).
(3) Simply changing the formation pattern on the first layer from the balanced circular to the uniform spacing pattern, an overall uniform spacing formation is obtained with local geometric shapes in triangles. The formation pattern is shown in Fig. 5(d).

To clarify how subgroups are defined, how the leader of each subgroup is chosen, and if the robots know the size of their subgroups a priori, we use Fig. 5(a) as an example. For the subgroup consisting agents {1, 2, 3}, members in this subgroup are defined by specifying agent 1 not to "seek" anyone else; agent 2 "seeking" agent 1; and agent 3 "seeking" agent 2. In each subgroup, all members do not know the total number of that subgroup a priori. The "leader" only knows that it does not need to "seek" anyone else in its subgroup. The rest of the members only know which one to "seek". In the simulation examples, the knowledge of which agent to "seek" is assigned. In reality, these knowledges can be perceived by the agents so that formation can still be maintained with agents joining or leaving the group.

At this point, we would like to highlight differences between the control laws of previous work [35], [36] and the new work in this paper, *i.e.*, formation controllers (6), (7), (16), and (17), as well as discussing some interesting aspects of the new control laws. Three formation controllers were reported in [35], [36] each achieving a balanced circular formation under one of the following three communication topologies: (1) all-to-all, (2) ring, and (3) cyclic pursuit. Using the balanced circular formation, all agents, which circle on the same orbit around the target, spread evenly around a full circle, whose centre resides in the moving target. These previous works are focused on studying the feasibility of achieving formations for target tracking. Having successfully obtained cooperative tracking in the balanced circular formation, one would naturally wonder what other formation patterns can be obtained that also fit into the tracking scenario. Instead of spreading all agents over one full circle, spreading them over a portion of a circle (*i.e.*, an arc) is one natural variation. Two uniform spacing formation controllers (6) and (7) are presented in this paper. Controller (6), adopted from [32], is adapted into the chain-type communication topology. Controller (7) that is expressed as a function of the relative bearing angle(s) $\beta_{ij}(t)$ alone is proposed in this paper. Controller (7) regulates the separation angles between a pair of agents, instead of the separation distances between them as in (6). The difference between regulating separation distances and separation angles is not obvious when UAVs circle on the same orbit because a constant separation distance is equivalent to a constant separation angle under this circumstance.

However, when agents circle on different orbits (circles of different radii around the target), the difference is clear, as to be demonstrated in Figs. 6 and 7. By properly specifying the desired 2D ranges and setting the UAV's linear velocities accordingly, UAVs can now be controlled to circle on different orbits. With this feature in place, uniform spacing formations are achieved by using the virtual agent to represent an actual agent in need. Controllers (6) and (7) are modified to use relative bearing angles $\tilde{\beta}_{i,j}(t)$ referring to the virtual agent(s), yielding new controllers (16) and (17) for the case of circling on different orbits.

The ultimate objective is to achieve more versatile concentric formation patterns, such as patterns with local geometric shapes. This is made possible utilizing existing works (tracking [38], balanced circular formation [35], [36]) and the new results presented in this paper (uniform spacing formations that regulate either separation distances or angles for agents circling on the same or different orbits, and hierarchy). Results presented in this paper provide more complete solution to cooperative target tracking in concentric formations, by designing the control input of each UAV as a sum of several individual control components. One practical issue of avoiding inter-vehicle collision is to be addressed in Section 5. The combination of Attraction (another way of saying tracking), Alignment (formation), and Avoidance (collision avoidance) provides a solid framework to achieve formations in the context of target tracking.

Another advantage of having versatile formation patterns is that it can possibly allow agents to acquire information of each other using a mixture of information exchange (over communication channels, for agents that are far away) and onboard sensing/perception (for agents that are close to each other). Refer to the two patterns in Fig. 5(a) and (c), where overall balanced circular formations have been achieved with local geometric shapes of either straight lines or triangles. The "leaders" of the three subgroups, can exchange information over the communication channels because they are relatively far away and might not be able to "see" each other. The other two members of each subgroup can possibly use onboard sensing to obtain the information; they need to achieve local formations (because they are close and can perceive each other).

5. Inter-vehicle Collision Avoidance

When developing the uniform spacing formation, collision between UAVs is more likely to occur than other patterns where agents are far away from each other. A strategy

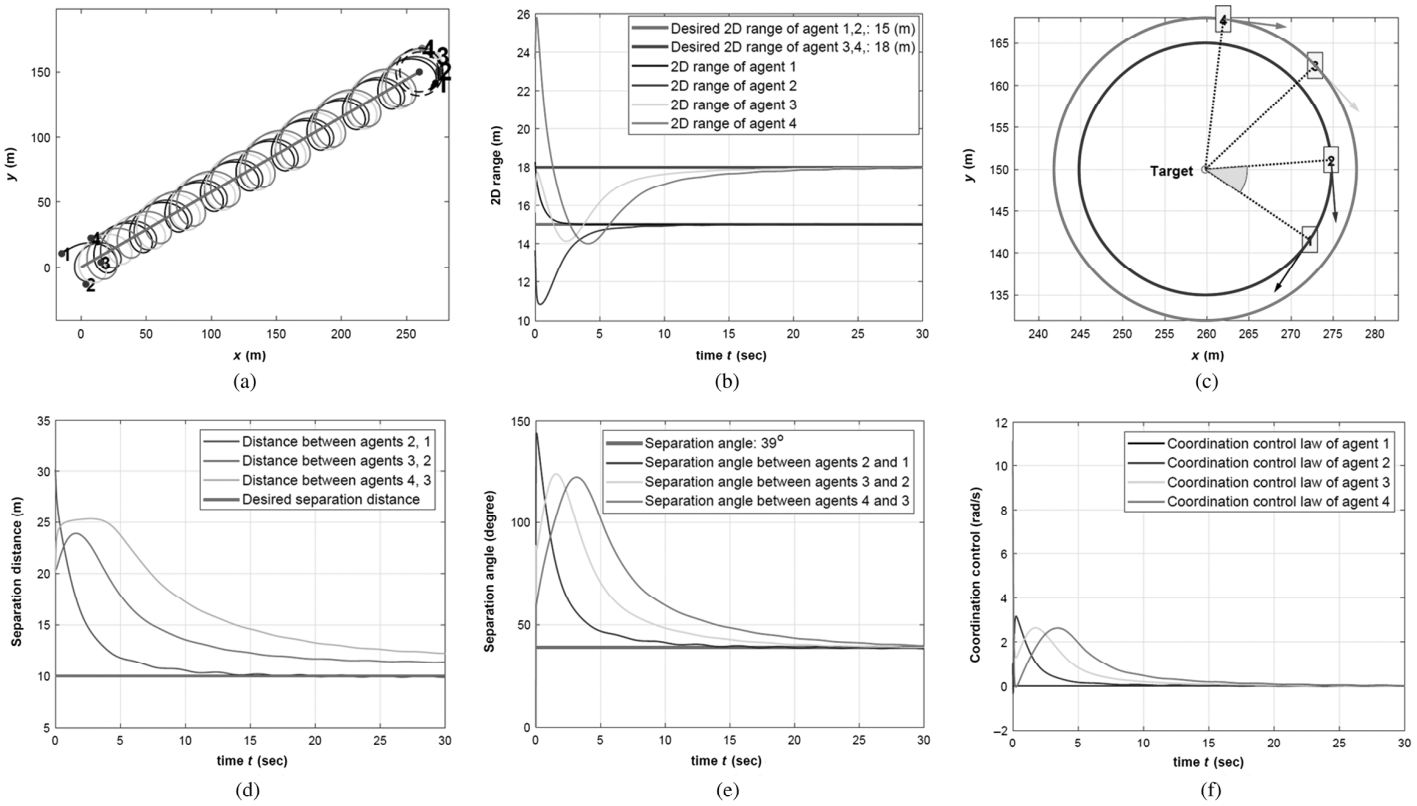

Figure 6. Cooperative target tracking using formation controller (17): (a) 2D trajectories; (b) 2D range; (c) formation in the end; (d) separation distance; (e) separation angle; and (f) formation control $u_{ic}(t)$. Target undergoes a linear motion. Agents circle on two different orbits.

of preventing the inter-vehicle collision is thus much in demand. Among methods that prevent collisions, one way is to apply a force that repels the agents once they get closer. This force should also be strong enough to defend other forces pushing agents to a collision [45]–[49].

Let $d_{\min}$ denote the minimal distance allowed among agents. The following collision avoidance control component helps to repel agents to steer away from each other once they get too close [50]:

$$u_{ia}(t) = -K_r \sum_{j \in \mathcal{N}(r_i)} \frac{d_{\min}}{d_{ij}} \sin \beta_{ij} \tag{18}$$

where K_r is the controller gain. The repulsion term (18) adjusts each agent's heading to the opposite direction of its neighbours in $\mathcal{N}(\boldsymbol{r}_i)$. Notice that $\mathcal{N}(\boldsymbol{r}_i)$ and $\mathcal{N}_i$ denote different sets. The set $\mathcal{N}_i$ is the set of agents whose information can be obtained by the ith agent *via* communication, whereas the set $\mathcal{N}(\boldsymbol{r}_i)$ denotes the set of agents that are too close to agent i.

With (18) in place, each agent's control input becomes [50]:

$$\dot{\psi}_i(t) = u_i(t) = u_{it}(t) + u_{ic}(t) + u_{ia}(t) \tag{19}$$

Totally three control components are added together to achieve the objective of simultaneous tracking, formation, and inter-vehicle collision avoidance.

6. Simulation Results

The proposed control laws were simulated in Matlab to verify their performance of tracking, formation, and inter-vehicle collision avoidance.

6.1 Achieving Uniform Spacing Formations on Different Orbits

This example demonstrates achievement of uniform spacing formations when agents circle on different orbits. To achieve formations under this circumstance, formation controllers (17) and (16) are used, which resort to virtual agents when needed, *i.e.*, when the two agents are not on the same orbit. It is worth mentioning that the formation controller (16) aims at regulating the relative separation distances to a constant, while the controller (17) regulates the relative separation angles to a desired value. The 2D ranges are set to be $\rho_{d,i} = \{15, 15, 18, 18\}$ (m), for $i = 1, 2, 3, 4$, respectively. Correspondingly, UAVs' linear velocities are $V_{g,i} = \{30, 30, 36, 36\}$ (m/s), satisfying the relationship in (10). To focus on the formation patterns, the target's motion is assumed linear (the target moves on a straight line).

We first present simulation results applying the formation controller (17). The 2D trajectories of the agents and the target are plotted in Fig. 6(a). Details of the tracking are given in Fig. 6(b), where $\rho_i(t)$ approach their prescribed values (that are different). All agents' positions at the end of the simulation are shown in Fig. 6(c),

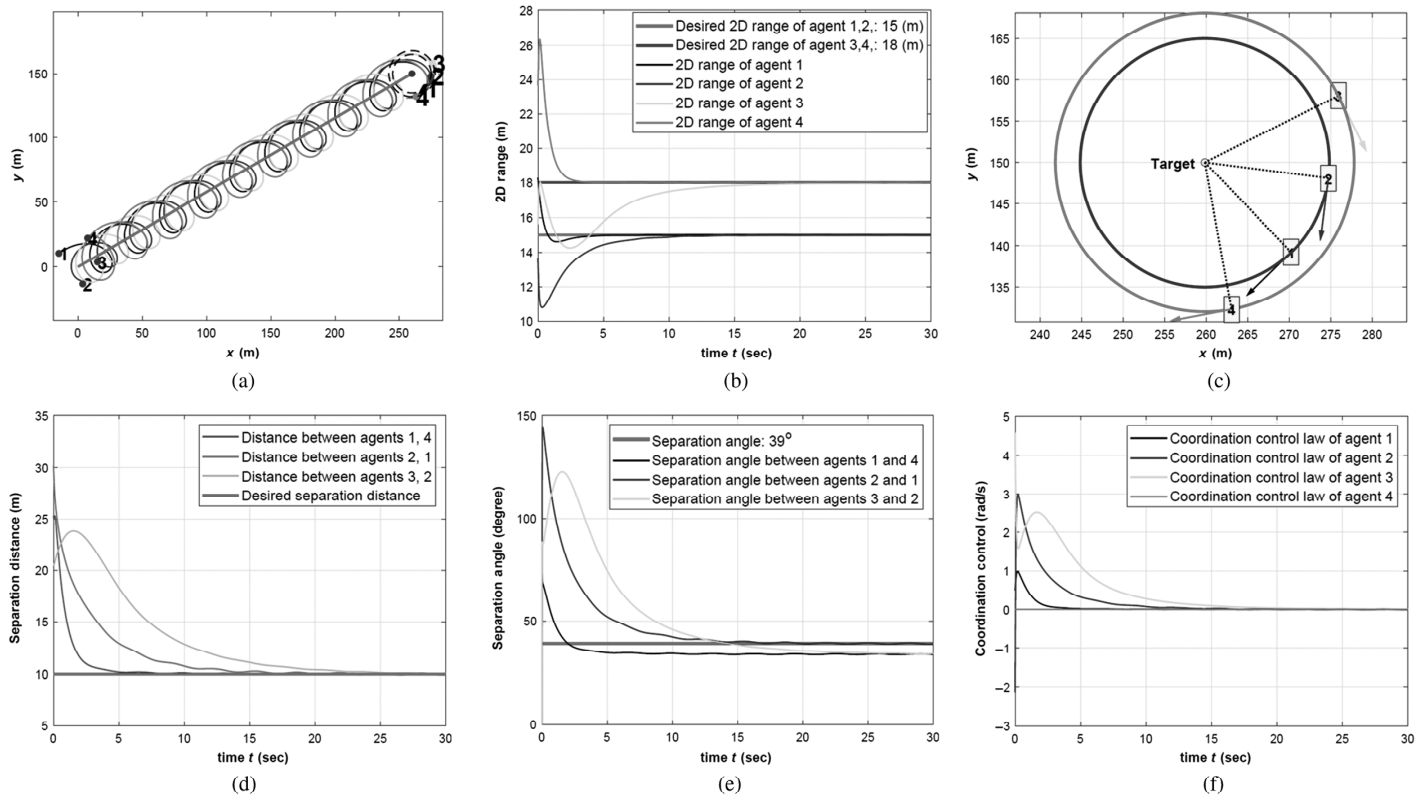

Figure 7. Cooperative target tracking using formation controller (16): (a) 2D trajectories; (b) 2D range; (c) formation in the end; (d) separation distance; (e) separation angle; and (f) formation control $u_{ic}(t)$. Target undergoes a linear motion. Agents circle on two different orbits.

where all agents scatter around the target on two different orbits. Both the separation distances (Fig. 6(d)) and the separation angles (Fig. 6(e)) are plotted. When controller (17) is applied, we expect the separation angles to approach a constant. However, the separation distances may or may not approach to the same value because the distances between two agents also depend on the orbits that they lie on. For $d_s = 10\,(\mathrm{m})$, the desired separation angle is either $\phi_s = 2\sin^{-1}(d_s/30) \approx 39^\circ$ or $\phi_s = 2\pi - 2\sin^{-1}(d_s/30) \approx 321^\circ$. Because all separation angles converge to 39°(Fig. 6(e)), formation is obtained successfully. Figure 6(f) shows the formation component $u_{ic}(t)$, which converges to zero upon formation.

Results when applying the controller (16) are shown in Fig. 7. Figure 7(a) shows the general picture of cooperative target tracking. Figure 7(b) plots the 2D ranges between the agents and the target, demonstrating successful tracking with two different range values. Figure 7(c) shows the formation achieved in the end, where agents circle on two different orbits around the target. Figure 7(d) shows that the separation distances between two successive agents are now regulated to the specified value of $d_s = 10$ (m) (same for all agents). On the contrary, the separation angles do not approach to one value. From Fig. 7(c), it can be seen that agents $\{1, 4\}$ and agents $\{2, 3\}$ circle on two different orbits. The separation angles between these two pairs of consecutive agents should be smaller than that between agents $\{1, 2\}$, which circle on the same orbit. This is confirmed in Fig. 7(e). Figure 7(f) shows that the formation control component $u_{ic}(t)$ also vanishes to zero upon formation.

Figures 6 and 7 together show the difference between the two formation controllers (16) and (17). The formation controller (16) regulates the relative separation *distances* between agents to a specified value d_s, while the controller (17) regulates the separation *angles* to ϕ_s.

6.2 Achieving Concentric Formations with Local Geometric Shapes

This section presents cooperative target tracking in concentric formations with local geometric shapes of straight lines and triangles, as those shown in Fig. 5. To focus on formation patterns, the target's motion is assumed linear, *i.e.*, the target moves on a straight line. Corresponding to the four patterns in Fig. 5, simulation results are presented in Fig. 8, with several snapshots showing how formation is achieved over time. Cooperative target tracking in these concentric formations are successfully obtained.

6.3 Achieving Inter-vehicle Collision Avoidance

This example demonstrates cooperative target tracking with inter-vehicle collision avoidance. The two scenarios of *without* and *with* collision avoidance, *i.e.*, before and after applying $u_{ia}(t)$, are shown and compared in Fig. 9. We select the target's velocity to be piecewise-constant, $n = 5$, $d_s = 10$ (m), and $d_{\min} = 7$ (m). The first row of Fig. 9 is

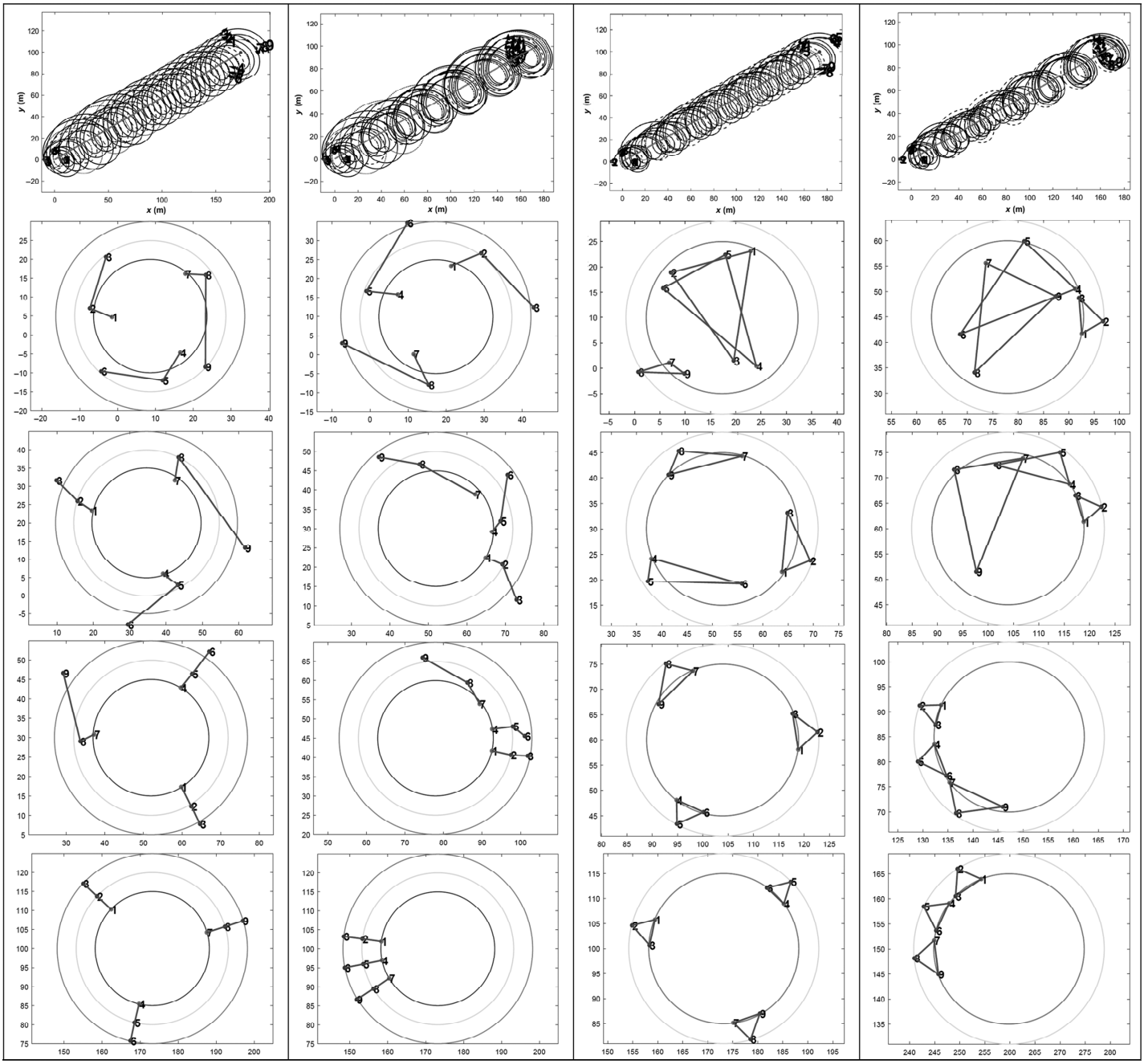

Figure 8. Cooperative target tracking in local geometric shapes: (a) balanced-line; (b) uniform-line; (c) balanced-triangle; and (d) uniform-triangle. The overall formation is either balanced circular or uniform spacing. The local geometric shape is either straight line or triangle.

for the scenario without the collision avoidance capability, *i.e.*, before the control component $u_{ia}(t)$ is applied. After $u_{ia}(t)$ is applied, results are shown in the second row of Fig. 9. In each scenario, the 2D trajectories are plotted to show the general picture (Fig. 9(a) versus (c)). Then, the minimal distance among all agents is plotted, demonstrating the effect of the added control component $u_{ia}(t)$ (Fig. 9(b) versus (d)). For the second scenario with collision avoidance, the component $u_{ia}(t)$ for each agent is shown in Fig. 9(e), where a saturation of $|u_{ia}(t)| \leq 3$ has been used for all agents. Comparison between Fig. 9(b) and (d) shows that the control component $u_{ia}(t)$ helps to keep the minimal distance to be greater than the allowed value. Otherwise, the minimal distance can be much smaller, as indicated in Fig. 9(b). The zigzag area in Fig. 9(d), corresponds to the circumstances when $u_{ia}(t)$ takes effect. Figure 9(e) shows that $u_{ia}(t)$ only takes effect when needed, *i.e.*, when agents $\{3, 5\}$ get too close to each other.

7. Comparison with Prior Studies

Comparing with the distance-based coordination control law (6), our proposed bearing-angle-based coordination control law (7) has one potential advantage. Consider a

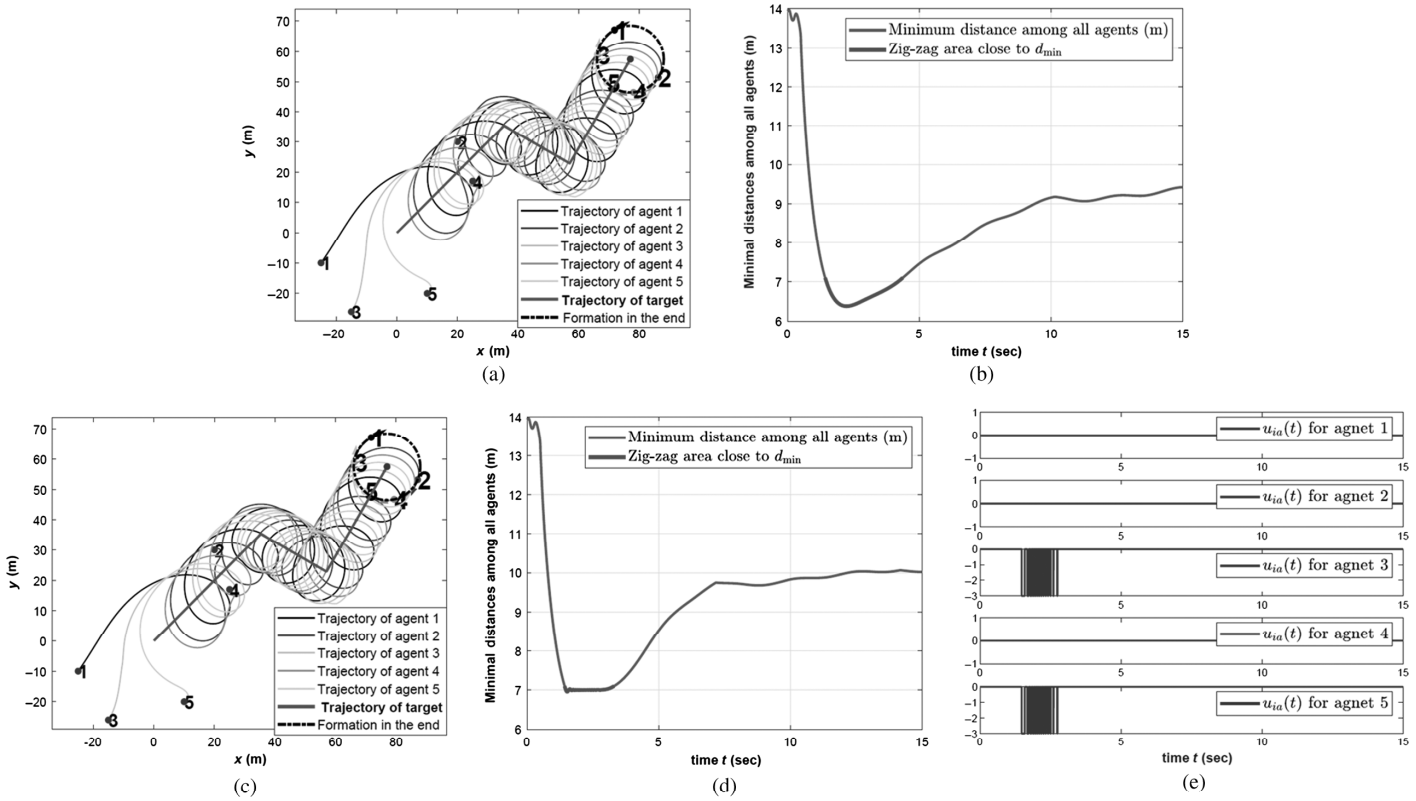

Figure 9. With inter-vehicle collision avoidance (before and after): (a) before 2D trajectories; (b) before minimum distance; (c) after 2D trajectories; (b) after minimum distance; and (e) after $u_{ic}(t)$ (rad/s).

scenario when information exchange among/between some agents becomes unavailable (*e.g.*, due to communication loss or out of communication range). Instead of computing the relative bearing angles from the exchanged positions as in (12), the needed information of relative bearing angles can be estimated/obtained from a local vision system installed on each UAV. In other words, when the expected information from others is unavailable (either permanently or temporarily), the objective of achieving and maintaining formation could still be achieved by using local measurements and estimates.

Regarding formation control, most existing results are either leaderless or leader-following [51], [52]. The proposed method of obtaining versatile formation patterns allows a combination of both. This can be seen in the "Balanced-Line" and "Balanced-Triangle" patterns (Fig. 5). The overall balanced circular formation can be obtained using a leaderless communication topology, whereas achievement of local geometric shapes can be implemented in a leader-based manner. The adopted hierarchical formation structure allows selection of appropriate communication topologies on different layers.

This paper also considers a practical issue that would occur, *i.e.*, collisions among agents. This issue was tackled by adding another control component into each UAV's control input. As can be seen from (18), this added collision-avoidance control component can also be expressed as a function of bearing angles. As mentioned earlier, a bearing-angle-based control law has the potential of still achieving its control objective (formation or collision avoidance) during communication loss, by using local measurements from each UAV's onboard sensors.

8. Conclusions

This paper is to obtain more versatile concentric formations in cooperative target tracking where a fleet of UAVs is commanded to circle above (and around) a moving ground target. On the basis of our previous results, versatile formation patterns are achieved with the help of three new features. The first feature is a new formation pattern, the uniform spacing formation where either the relative separation distances or the separation angles can be regulated to a desired value. Different from a balanced circular formation where agents spread evenly over a full circle, agents can now spread evenly over a portion of a circle. Two kinds of uniform spacing formation control laws are proposed, where one regulates the separation distances between two agents and the other regulates the separation angles in between. The second feature allows UAVs to circle on different orbits. To achieve formation under this circumstance, formation controllers will resort to virtual agents representing the actual agents in need. The third feature is the usage of a (two-layer) hierarchical formation structure, which allows selection of formation patterns for different layers. Combinations of these new features with our existing results yield more versatile concentric formation patterns with different local geometric shapes, such as straight lines and triangles. Inter-vehicle collision avoidance is also addressed. Agents will be repelled to steer away from each other once they get too close.

All UAVs are assumed to have constant linear velocities. Control of each UAV is *via* its yaw rate. The design idea is to add three control components (three heading controllers) together to achieve the overall objective. Each control component has a goal. The proposed extensions to spreading agents on a portion of a circle, circling agents on orbits of different radii, formation in local geometric shapes, and avoiding inter-vehicle collisions, provide more complete solution to cooperative target tracking in the concentric manner.

This paper also raises several questions for future investigations. The implementation of the proposed schemes on physical robots and the extension of the developed techniques to 3D scenarios and cooperative tracking of multiple targets with obstacle avoidance capability [53], [54] will be of particular interest. Stability analyses in the presence of formation pattern switching and broken communication links are another research direction to look into. Also, investigations of the time delay factor for obtaining stability conditions as well as desirable performance with reasonable computation complexity [55]–[57] are needed. Finally, Artificial Intelligence (AI) techniques have recently been developed for robotic communication to enhance the communication capability of robotic networks for coordinated actions. Application of the AI and/or Neural Networks to the field of robotic networks in the context of cooperative target tracking is a promising research area to pursue [58]–[60].

References

[1] K. Szwaykowska, I.B. Schwartz, L.M.-T. Romero, C.R. Heckman, D. Mox, and M.A. Hsieh, Collective motion patterns of swarms with delay coupling: Theory and experiment, *Physical Revie E*, *93*(3), 2016, 11.

[2] R. Sepulchre, D. Paley, and N. Leonard, Stabilization of planar collection motion: All-to-all communication, *IEEE Transactions on Automatic Control*, *52*(5), 2007, 811–824.

[3] R. Sepulchre, D. Paley, and N. Leonard, Stabilization of planar collective motion with limited communication, *IEEE Transactions on Automatic Control*, *53*(3), 2008, 706–719.

[4] A. Jain, D. Ghose, and P. Menon, Stabilization of balanced circular motion about a desired center, *International Conference on Advances in Control and Optimization of Dynamical Systems*, Kanpur, India, 2014.

[5] A. Jain and D. Ghose, Stabilization of collective motion in synchronized, balanced and splay phase arrangements on a desired circle, *American Control Conference*, Chicago, IL.

[6] G. Mallik and A. Sinha, A study of balanced circular formation under deviated cyclic pursuit strategy, *IFAC-PapersOnLine*, *48*(5), 2015, 41–46.

[7] R. Zheng, Z. Lin, M. Fu, and D. Sun, Distributed control for uniform circumnavigation of ring-coupled unicycles, *Automatica*, *53*, 2015, 23–29.

[8] N. Kokolakis and N. Koussoulas, Coordinated standoff tracking of a ground moving target and the phase separation problem, *International Conference on Unmanned Aircraft Systems*, Dallas, TX, 2018.

[9] J. Guo, G. Yan, and Z. Lin, Cooperative control synthesis for moving-target-enclosing with changing topologies, *International Conference on Robotics and Automation*, Anchorage, AK, 2010.

[10] Z. Zhou, H. Wang, and Z. Hu, Event-based time varying formation control for multiple quadrotor UAVs with Markovian switching topologies, *Complexity,* 2018, 1–15.

[11] Y. Sun and L. Wang, Consensus of multi-agent systems in directed networks with nonuniform time-varying delays, *IEEE Transactions on Automatic Control*, *54*(7), 2009, 1607–1613.

[12] J. Marshall, M. Broucke, and B. Francis, Formations of vehicles in cyclic pursuit, *IEEE Transactions on Automatic Control*, *49*(11), 2004, 1963–1974.

[13] J. Marshall, M. Broucke, and B. Francis, Pursuit formations of unicycles, *Automatica*, *42*, 2006, 3–12.

[14] M. Pavone and E. Frazzoli, Decentralized policies for geometric pattern formation and path coverage, *ASME Journal of Dynamic Systems, Measurement, and Control*, *129*(5), 2007, 633–643.

[15] B. Wu, D. Wang, and E. Poh, Cyclic formation control for satellite formation using local relative measurements, *Mechatronic Systems and Control*, *40*(1), 2012, 11–21.

[16] J. Juang, On the formation patterns under generalized cyclic pursuit, *IEEE Transactions on Automatic Control*, *58*(9), 2013, 2401–2405, 2013.

[17] J. Ramirez, M. Pavone, E. Frazzoli, and D. Miller, Distributed control of spacecraft formations via cyclic pursuit: Theory and experiments, *Journal of Guidance, Control, and Dynamics*, *33*(5), 2010, 1655–1669.

[18] K. Hausmany, J. Muller, A. Hariharan, N. Ayanian, and G. Sukhatme, Cooperative multi-robot control for target tracking with onboard sensing, *International Journal of Robotics Research*, *34*(13), 2015, 1660–1677.

[19] P. Jimenez, B. Shirinzadeh, D. Oetomo, and A. Nicholson, Swarm aggregation and formation control for robots with limited perception, *International Journal of Robotics and Automation*, *26*(4), 2011, 255–263.

[20] P. Zhu and W. Ren, Multi-robot joint localization and target tracking with local sensing and communication, *American Control Conference*, Charlotte, NC, 2019.

[21] L. Luo, N. Chakraborty, and K. Sycara, Provably-good distributed algorithm for constrained multi-robot task assignment for grouped tasks, *IEEE Transactions on Robotics*, *31*(1), 2015, 19–30.

[22] D. Panagou, M. Turpin, and V. Kumar, Decentralized goal assignment and safe trajectory generation in multi-robot networks via multiple Lyapunov functions, *IEEE Transactions on Automatic Control*, *65*(8), 2020, 3365–3380.

[23] J. Ni, X. Yang, J. Chen, and S. Yang, Dynamic bioinspired neural network for multi-robot formation control in unknown environments, *International Journal of Robotics and Automation*, *30*(3), 2015, 256–266.

[24] M. Khan and C. Silva, Autonomous and robust multi-robot cooperation using an artificial immune system, *International Journal of Robotics and Automation*, *27*(1), 2012, 60–75.

[25] X. Yu, L. Liu, and G. Feng, Coordinated control of multiple unicycles for escorting and patrolling task based on a cyclic pursuit strategy, *American Control Conference*, Boston, MA, 2016.

[26] M. Zhang and H. Liu, Cooperative tracking a moving target using multiple fixed-wing UAVs, *Journal of Intelligent and Robotic Systems*, *81*(3-4), 2016, 505–529.

[27] X. Yu and L. Liu, Cooperative control for moving-target circular formation of nonholonomic vehicles, *IEEE Transactions on Automatic Control*, *62*(7), 2017, 3448–3454.

[28] L. Brinon-Arranz, A. Seuret, and A. Pascoal, Target tracking via a circular formation of unicycles, *IFAC World Congress*, Toulouse, France, 2017.

[29] A. Miao, Y. Wang, and R. Fierro, Cooperative circumnavigation of a moving target with multiple nonholonomic robots using backstepping design, *Systems and Control Letters*, *103*, 2017, 58–65.

[30] L. Ma and N. Hovakimyan, Vision-based cyclic pursuit for cooperative target tracking, *Journal of Guidance, Control, and Dynamics*, *36*(2), 2013, 617–622.

[31] N. Moshtagh, N. Michael, A. Jadbabaie, and K. Daniilidis, Vision-based, distributed control laws for motion coordination of nonholonomic robots, *IEEE Transactions on Robotics*, *25*(4), 2009, 851–860.

[32] N. Ceccarelli, M. Marco, A. Garulli, and A. Giannitrapani, Collective circular motion of multi-vehicle systems, *Automatica*, *44*, 2008, 3025–3035.

[33] J. Soares, A. Aguiar, A. Pascoal, and M. Gallieri, Triangular formation control using range measurements: An application to marine robotic vehicles, *IFAC Proceedings*, *45*(5), 2012, 112–117.

[34] Z. He and J. Xu, Moving target tracking by UAVs in an urban area, *Mechatronic Systems and Control*, *42*(2), 2014. DOI: 10.2316/Journal.201.2014.2.201-2572.

[35] L. Ma and N. Hovakimyan, Cooperative target tracking in balanced circular formation: Multiple UAVs tracking a ground vehicle, *American Control Conference*, Washington, DC, USA, 2013, 5386–5391.

[36] L. Ma, Cooperative target tracking with time-varying formation radius, *European Control Conference*, Linz, Austria, 2015.

[37] L. Ma, Cooperative target tracking in balanced circular formation with time-varying radius, *International Journal of Robotics and Automation*, *35*(4), 2020. DOI: 10.2316/J.2020.206-0086.

[38] L. Ma, C. Cao, N. Hovakimyan, V. Dobrokhodov, and I. Kaminer, Adaptive vision-based guidance law with guaranteed performance bounds, *Journal of Guidance, Control, and Dynamics*, *3*, 2010, 33.

[39] V. Cichella, I. Kaminer, V. Dobrokhodov, and N. Hovakimyan, Coordinated vision-based tracking for multiple UAVs, *American Control Conference*, Hamburg, Germany, 2015.

[40] Q. Han, S. Sun, and H. Lang, Leader-follower formation control of multi-robots based on bearing-only observations, *International Journal of Robotics and Automation*, *34*(2), 2019. DOI: 10.2316/J.2019.206-4831.

[41] S. Smith, M. Broucke, and B. Francis, A hierarchical cyclic pursuit scheme for vehicle networks, *Automatica*, *41*, 2005, 1045–1053.

[42] L. Consolini, F. Morbidi, D. Prattichizzo, and M. Tosques, Steering hierarchical formations of unicycle robots, *IEEE Conference on Decision and Control*, New Orleans, LA, 2007.

[43] D. Mukherjee and D. Ghose, Generalized hierarchical cyclic pursuit, *Automatica*, *71*, 2016, 318–323.

[44] W. Ding, G. Yan, and Z. Lin, Formations on two-layer pursuit systems, *IEEE International Conference on Robotics and Automation*, Japan, 2009.

[45] A. Satici, H. Poonawala, H. Eckert, and M. Spong, Connectivity preserving formation control with collision avoidance for nonholonomic wheeled mobile robots, *IEEE International Conference on Intelligent Robots and Systems*, Tokyo, Japan, 2013.

[46] J. Santiaguillo-Salinas and E. Arando-bricaire, Containment problem with time-varying formation and collision avoidance for multiagent systems, *International Journal of Advanced Robotic Systems*, *13*, 2017, 1–13.

[47] J. Flores-Resendiz, E. Aranda-Bricaire, J. González-Sierra, and J. Santiaguillo-Salinas, Finite-time formation control without collisions for multiagent systems with communication graphs composed of cyclic paths, *Mathematical Problems in Engineering*, *1*, 2015, 1–17.

[48] V. Freitas and E. Macau, Control strategy for symmetric circular formations of mobile agents with collision avoidance, *FHYSCON*, Florence, Italy, 2017.

[49] A. Burohman, E. Joelianto, and A. Widyotriatmo, Analysis of potential fields for formation of multi-agent robots with collision avoidance, *International Conference on Instrumentation, Control, and Automation*, Yogyakarta, Indonesia, 2017.

[50] L. Ma, Cooperative target tracking using a fleet of UAVs with collision and obstacle avoidance, *International Conference on System Theory, Control and Computing*, Sinaia, Romania, 2018.

[51] X. Ma, W. Dong, and B. Li, Comprehensive fault-tolerant control of leader-follower unmanned aerial vehicles (UAVs) formation, *International Journal of Robotics and Automation*, *34*(6), 2019. DOI: 10.2316/J.2019.206-0301.

[52] D. Atta and B. Subudhi, Decentralized formation control of multiple autonomous underwater vehicles, *International Journal of Robotics and Automation*, *28*(4), 2013. DOI: 10.2316/Journal.206.2013.4.206-3613.

[53] L. Deng, X. Ma, J. Gu, Y. Li, Z. Xu, and Y. Wang, Artificial immune network-based multi-robot formation path planning with obstacle avoidance, *International Journal of Robotics and Automation*, *31*(3), 2016. DOI: 10.2316/Journal.206.2016.3.206-4746.

[54] A. Abbaspour, A. Moosavian, and K. Alipour, Formation control and obstacle avoidance of cooperative wheeled mobile robots, *International Journal of Robotics and Automation*, *30*(5), 2015. DOI: 10.2316/Journal.206.2015.5.206-4109.

[55] Z. Li, H. Yan, H. Zhang, X. Zhan, and C. Huang, Improved inequality-based functions approach for stability analysis of time delay system, *Automatica*, *108*, 2019, 108416.

[56] Z. Li, H. Yan, H. Zhang, Y. Peng, J. Park, and Y. He, Stability analysis of linear systems with time-varying delay via intermediate polynomial-based functions, *Automatica*, *113*, 2019, 108756.

[57] Z. Li, C. Huang, and H. Yan, Stability analysis for systems with time delays via new integral inequalities, *IEEE Transactions on Systems, Man, and Cybernetics: Systems*, *48*(12), 2018, 2495–2501.

[58] Z. Li, Y. Bai, C. Huang, H. Yan, and S. Mu, Improved stability analysis for delayed neural networks, *IEEE Transactions on Neural Networks and Learning Systems*, *29*(9), 2017, 4535–4541.

[59] Z. Li, H. Yan, H. Zhang, X. Zhan, and C. Huang, Stability analysis for delayed neural networks via improved auxiliary polynomial-based functions, *IEEE Transactions on Neural Networks and Learning Systems*, *30*(8), 2019, 2562–2568.

[60] Z. Li, H. Yan, H. Zhang, J. Sun, and H. Lam, Stability and stabilization with additive freedom for delayed Takagi–Sugeno fuzzy systems by intermediary-polynomial-based functions, *IEEE Transactions on Fuzzy Systems*, *28*(4), 2020, 692–705.

Biography

Lili Ma received her Ph.D. in Electrical Engineering from Utah State University focusing on autonomous ground vehicles. After that she did three-year postdoctoral training at Virginia Tech working with autonomous aerial vehicles. Prior to joining the Computer Engineering Technology Department at New York City College of Technology, she taught at Wentworth Institute of Technology for many years. Her research areas include autonomous robots, vision-based control, visual servoing, visual tracking, coordinated control, and sensing and perception techniques.